Rab3A negatively regulates activity-dependent modulation of exocytosis in bovine adrenal chromaffin cells

Ramachandran Thiagarajan[1], Teclemichael Tewolde[1], Yingjie Li[2], Peter L. Becker[1], Mark M. Rich[1,2] and Kathrin L. Engisch[1]

[1]*Departments of Physiology and* [2]*Neurology, Emory University School of Medicine, Atlanta, GA 30322, USA*

Members of the Rab family of monomeric GTPases have been implicated in vesicle trafficking, and Rab3A, located on synaptic vesicles in neurones and secretory vesicles in neuroendocrine cells, is likely to be involved in vesicle fusion leading to neurotransmitter release. A hydrolysis-deficient mutant of Rab3A, Rab3AQ81L, has been shown to potently inhibit hormone release. Here we show that the inhibition of hormone release by Rab3AQ81L is activity-dependent. Bovine adrenal chromaffin cells were induced to express Rab3AQ81L and green fluorescent protein by adenoviral gene transfer of a bicistronic construct. Fluorescent cells were stimulated with single depolarizations and trains of depolarizing pulses in whole cell perforated patch clamp recordings, and exocytosis was detected with cell capacitance measurements and carbon fibre amperometry. When single depolarizations were used to evoke exocytosis, cells expressing Rab3AQ81L showed a 50% reduction in response amplitude. When trains of brief depolarizations (10 or 40 ms) were used to evoke exocytosis, responses rapidly declined to zero in cells expressing Rab3AQ81L. Wild-type Rab3A had effects similar to Rab3AQ81L, causing significant inhibition of exocytosis only during repetitive stimulation. Expression of Rab5A did not alter exocytosis evoked by single depolarizations or repetitive stimulation. Applying a long duration depolarization in the middle of a stimulus train revealed that exocytotic efficacy (capacitance increase per amount of calcium influx) was not decreased in Rab3AQ81L-expressing cells. Instead, the activity-dependent increase in exocytotic efficacy observed in control cells did not occur in Rab3AQ81L-expressing cells. Our results suggest that Rab3A in the GTP bound conformation prevents activity-dependent facilitation.

(Received 3 October 2003; accepted after revision 16 December 2003; first published online 23 December 2003)
Corresponding author K. L. Engisch: Department of Physiology, Emory University School of Medicine, 605-J Whitehead Research Building, 615 Michael Street, Atlanta, GA 30322, USA. Email: kengisch@physio.emory.edu

Rab proteins are low molecular weight GTPases that regulate vesicle trafficking throughout the secretory and endocytic pathways. Rabs have been shown to participate in the movement of vesicles along cytoskeletal elements, to interact with tethering and docking factors, and to control the duration of the fusion event (see Zerial & McBride, 2001 for review). Transmitter release is a specialized form of vesicle trafficking in which synaptic vesicles are triggered to fuse with the plasma membrane by an influx of calcium ions. Rab3A is located on synaptic vesicles (Fischer von Mollard *et al.* 1990; Darchen *et al.* 1995; Schluter *et al.* 2002) and is likely to play an important role in transport, tethering, docking and/or fusion of synaptic vesicles. Despite significant progress in the field of Rab GTPases, the role of Rab3A in transmitter release has not been determined.

Rab3A is an unusual GTPase that may inhibit rather than promote vesicle trafficking. A Rab3A mutant, Rab3AQ81L, thought to be in the GTP-bound conformation due to loss of intrinsic GTPase activity (Brondyk *et al.* 1993) and responsiveness to a GTPase-activating protein (Rab3-GAP; Clabecq *et al.* 2000), inhibits hormone release by 50–80% when expressed in neuroendocrine cells (Holz *et al.* 1994; Johannes *et al.* 1994; Regazzi *et al.* 1996; Weber *et al.* 1996). Rab3AQ81L is likely to be the activated form of Rab3A since transmitter release is also reduced in bovine chromaffin cells expressing wild-type Rab3A (Holz *et al.* 1994).

If Rab3A is an inhibitory GTPase, its loss should lead to an increase in transmitter release, but this was not observed in either the *C. Elegans* Rab3 null mutant (Nonet *et al.* 1997) or the Rab3A-knockout mouse (Geppert *et al.* 1994).

 DOI: 10.1113/jphysiol.2003.056333

The only effects were changes in several forms of activity-dependent modulation, including paired pulse facilitation, train facilitation, and an adenylate cyclase-dependent form of LTP (Geppert *et al.* 1994; Castillo *et al.* 1997; Geppert *et al.* 1997; Castillo *et al.* 2002; Hirsh *et al.* 2002; Schoch *et al.* 2002).

We set out to understand how strong inhibition of release in the presence of the Rab3AQ81L mutant is related to the changes in activity-dependent modulation that occur in the Rab3A-knockout mouse. The overexpression studies that demonstrated the inhibitory effects of Rab3AQ81L and Rab3A could not distinguish whether transmitter release itself was inhibited, or if activity-dependent modulation was altered, because they measured hormone release over a 1–20 min period. A secretagogue such as a cholinergic agonist or raised potassium can trigger repetitive action potentials in adrenal chromaffin cells (Brandt *et al.* 1976; Nassar-Gentina *et al.* 1988; Zhou & Misler, 1995), which will cause modulation of release (Zhou & Misler, 1995; Seward & Nowycky, 1996; Engisch *et al.* 1997; Smith, 1999).

We stimulated bovine adrenal chromaffin cells expressing Rab3AQ81L with single and repetitive depolarizations in perforated patch clamp recordings, and detected exocytosis as increases in membrane surface area with capacitance detection. In some experiments, catecholamine release was also detected with a carbon fibre electrode. We report that Rab3AQ81L and wild-type Rab3A inhibit exocytosis primarily by preventing positive modulation during repetitive stimulation. A model for how Rab3A participates in activity-dependent modulation is discussed.

Methods

Plasmids

Plasmids for Rab3A and Rab3AQ81L, both tagged at the N-terminus with haemaglutinin (HA), were provided by Ian Macara (University of Virginia, Charlottesville). Plasmid for Rab5A was originally provided by Marino Zerial (Max Planck Institute of Molecular Cell Biology and Genetics, Dresden) and modified with an EGFP tag at the N-terminal in the laboratory of Allan Levey (Emory University, Atlanta).

Construction of adenoviruses

The pCI plasmid containing the CMV promoter/enhancer and an SV40 polyadenylation sequence flanked by adenovirus backbone was modified by inserting an internal ribosomal entry site (IRES) and the sequence for green fluorescent protein (GFP) as previously described (Gonzalez *et al.* 1999; Kraner *et al.* 1999). cDNAs encoding transgenes were cloned into the modified plasmid, and the entire fragment was cloned into the pAd-Link plasmid. Replication-defective, E1a-deleted adenoviruses containing the transgenes were generated by homologous recombination of the pAd-Link plasmid constructs with the Ad5 dL327 adenovirus backbone in human embryonic kidney 293 cells. GFP-positive plaques were selected, screened by Southern blot and purified as previously described (Kraner *et al.* 1999).

Preparation and culture of bovine chromaffin cells

Chromaffin cells were isolated from adult bovine adrenal glands obtained from a local abattoir (Bartow Meats, Cartersville, GA, USA) according to published procedures (Vitale *et al.* 1991; Engisch *et al.* 1999*a*). Chromaffin cells were purified on a Percoll gradient and plated at a density of 1.1×10^5 cells ml^{-1} on 12 mm glass coverslips coated with rat tail collagen. Cells were maintained in a 5% CO_2 humid atmosphere at 37°C in Dulbecco's modified Eagle's medium (DMEM) containing 25 mmol l^{-1} Hepes, 10% heat-inactivated fetal bovine serum (FBS), 0.01% streptomycin, 0.01% penicillin, 0.001% gentamycin, 10 μM cytosine arabinoside and 10 μM fluoro-deoxyuridine. Antibiotics were obtained from Sigma-Aldrich (St Louis, MO, USA), culture media from Life Technologies (Grand Island, NY, USA), FBS from Mediatech (Herndon, VA, USA), and Percoll from Amersham Biosciences (Piscataway, NJ, USA).

Adenovirus infection of chromaffin cells

Cells were infected with adenovirus on day 3 of culture and electrophysiological recordings performed 48 h postinfection. Half of the culture medium was removed and replaced with an equal volume of diluted virus in fresh plating medium. Multiple virus dilutions were tested in each culture. We found the optimal dilution produced bright GFP-positive cells at the same time that ~1/3 of the cells had no detectable GFP. The EGFP-tagged Rab5A construct (EGFP = 'enhanced GFP') gives a brighter fluorescence signal than the GFP produced by the IRES constructs, for the same level of protein expression. We were concerned that we might mistakenly choose a viral dilution of the Rab5A–EGFP virus that had a lower number of infectious particles if we used the absolute brightness of bright cells as a gauge. However, the number of cells that did not internalize virus should be the same for a

given concentration of live virus, so instead we used the number of fluorescence-negative cells to achieve similar infection levels for viruses with IRES–GFP constructs and the Rab5A–EGFP virus. The maximal concentration of virus used was 1×10^5 plaque-forming units ml^{-1} (pfu ml^{-1}), but was usually $< 0.5 \times 10^5$ pfu ml^{-1}.

Electrophysiological recording of membrane capacitance (C_m) and inward currents ($I_{Na,Ca}$)

A coverslip containing bovine adrenal chromaffin cells was transferred to the recording chamber and perfused with extracellular solution at a rate of 2 ml min^{-1}. Standard extracellular solution consisted of (mmol l^{-1}): 130 NaCl, 2 KCl, 10 dextrose, 10 Na-Hepes, 1 $MgCl_2$, 5 $CaCl_2$, 5 *N*-methyl-D-glucamine (NMDG); pH adjusted to 7.2 with HCl; 295 mosmol l^{-1}. Extracellular solutions of different calcium concentrations were prepared by decreasing the amount of $CaCl_2$ and compensating with NMDG for the change in osmolarity. Different extracellular solutions were applied to a cell via a large bore, square capillary tube (Warner Instruments, Hamden, CT, USA) placed at a distance of $\sim$50−100 μm. The tube was connected to four gravity-fed reservoirs through a four-way valve. Standard extracellular solution was perfused through the tube until the valve was switched to another reservoir.

Pipettes were pulled from custom length micropipette glass (Drummond Scientific, Broomall, PA, USA) on a two-stage microelectrode puller (Narishige; Pacer Scientific, Los Angeles, CA, USA), coated with Sylgard (WPI, Sarasota, FL, USA), and fire-polished. Pipette resistances were 1–2 MΩ when filled with intracellular solution containing (mmol l^{-1}): 135 caesium glutamate (prepared by titrating glutamic acid with 1 mol l^{-1} CsOH), 10 Mops (morpholino propane sulphonic acid), 0.5 Na_4BAPTA, 9.5 NaCl. Perforation solution was prepared by adding 5–7 μl of a 125 mg ml^{-1} stock of amphotericin B in DMSO to 1.4 ml of intracellular solution, and homogenizing for 5–10 s on a Pro-250 homogenizer fitted with a 7 mm × 120 mm generator (Proscientific, Oxford, CT, USA). All salts were purchased from Sigma-Aldrich except CsOH (ICN, Costa Mesa, CA, USA) and amphotericin B (Sigma-Aldrich and Calbiochem, San Diego, CA, USA).

Capacitance measurements were performed with an Axopatch 200B patch clamp amplifier (Axon Instruments, Union City, CA, USA) equipped with a resistance dither circuit (DR-1). A sine wave stimulus (40 mV peak to peak) was added to the holding potential of −90 mV. The optimal phase angle for capacitance measurements was determined by a software-based phase tracking algorithm (Fidler & Fernandez, 1989; Engisch & Nowycky, 1996; Engisch *et al.* 1997). Ten sine waves were averaged for each capacitance and conductance point for a time resolution of 10 ms per point on a PC with a Pentium II 400 MHz processor. Capacitance changes were calibrated by activating a capacitance dither that increased membrane capacitance by 100 fF.

Inward currents (Na^+ and Ca^{2+}) evoked by depolarization were acquired at a sampling rate of 20 kHz for 10 and 40 ms pulses, 5 kHz for 160 ms pulses, and 2.5 kHz for 320 ms pulses. All currents were filtered at 5 kHz. Capacitance measurements and the sine wave input were suspended during depolarizations. Recordings were initiated when series resistance reached 15 MΩ; series resistance usually declined further and stabilized between 8 and 12 mΩ for the duration of the recording.

Measurements of intracellular calcium concentration

Cells were plated on collagen-coated glass bottom dishes (Mat-Tek, Ashland, MA, USA) and infected with control adenovirus or Rab3AQ81L adenovirus on day 3 as described above. On day 5, plating medium was replaced with Earle's balanced salt solution (EBSS, Sigma-Aldrich) containing 2 μm l^{-1} of the acetoxymethyl ester form of Fura-4F (Molecular Probes, Eugene, OR, USA) and returned to the incubator for 45–60 min at 37°C. The dish was rinsed 3 times with extracellular solution before placing on the stage of an inverted Zeiss Axiovert 10 fluorescence microscope; extracellular solution was continuously perfused at 1–2 ml min^{-1}. Cells were voltage clamped in the perforated patch mode with an Axopatch 1D patch clamp amplifier (Axon Instruments). Excitation light from a xenon lamp source was alternated via a motorized filter wheel containing transmissive wedges that pass 340, 380 and 470 nm light, spinning at 1 revolution every 9 ms. Emitted light (510–550 nm) was detected by a photomultiplier tube (PMT) connected to a custom-designed photon counter interfaced to a computer. Background fluorescence was minimized by stopping down the field diaphragm to its minimum, a perimeter slightly larger than the cell diameter. Signals were kept within the linear range of the photon counter using a neutral density filter. Fluorescence signals and current signals were simultaneously acquired using custom software as previously described (Laflamme & Becker, 1996). Background fluorescence at each wavelength was obtained after removal of the cell using the patch pipette; background was subtracted prior to calculating the 340/380 fluorescence ratio. Cells with PMT counts at 470 nm that were a minimum of 4 times the average level

for uninfected cells were accepted as 'bright' GFP-positive cells.

Amperometric detection of catecholamine release

Amperometry was performed as previously described (Engisch *et al.* 1997). Briefly, amperometric electrodes consisted of an 8 μm carbon fibre, cemented inside a glass micropipette using epoxy that was subsequently cured for 24 h at room temperature, 2 h at 100°C and 2 h at 150°C (Kawagoe *et al.* 1993). The carbon fibre tip was cut immediately prior to recording, and an electrode was used for multiple recordings by recutting the tip. The electrode was held at +780 mV using an Axon Axopatch 200B patch clamp amplifier. Electrodes were positioned close to or just touching the cell. Acquisition of amperometric currents was initiated by a trigger from the capacitance detection software at the onset of a stimulus train. Data were filtered at 5 kHz and sampled at 2.5 kHz.

Data analysis and statistics

Calcium influx in picocoulombs was determined by integrating the inward current in response to a depolarizing voltage step, using limits that excluded the major portion of inward Na^+ current. The validity of this approach was confirmed in experiments in which 200 μmol l^{-1} Cd^{2+} was applied to block calcium current (not shown). Current traces were digitally leak-subtracted prior to integration. Leak current was determined immediately before each stimulus by hyperpolarizing the cell to −110 mV for the same duration and scaling the response.

The capacitance jump was determined from the difference between the resting capacitance, an average calculated for 200 ms immediately preceding a stimulus, and an average for the 200 ms following the depolarization. To correct for a capacitance transient thought to be due to non-exocytotic sources (Horrigan & Bookman, 1994; Chow *et al.* 1996), a separate group of virus-infected cells were exposed to 200 μm l^{-1} cadmium (Chan & Smith, 2003) and stimulated with each protocol, a train of 10 ms pulses, a train of 40 ms pulses, and single depolarizations of 40, 160 and 320 ms. The capacitance traces from 12–15 cells were averaged for each protocol, and the capacitance jumps determined as described above. The amplitude determined from average traces in cadmium-perfused cells was subtracted from responses evoked by single depolarizations in Figs 3*E* and *F*, 4*C*, and 5*B*. We have subtracted the amplitude of the transient from the response to the first pulse of a train in Figs 1*C*, 2*C*, 4*A* and *B*, 5*A*, and 6*C*, because although the transient does not decline or inactivate during repetitive stimulation, the calculated capacitance jump is only non-zero for the first pulse. This is because each jump during a train is determined relative to the level of the previous jump, and the transient cancels out after the first pulse. The amplitude of poststimulus drift was taken as the difference between the capacitance jump and the peak poststimulus capacitance. For generating the calcium influx–exocytosis relationship, data for a given treatment (e.g. control, Rab3AQ81L virus) were sorted from the smallest to largest amount of calcium influx, and grouped into bins. The average calcium influx and capacitance change for each bin are plotted in Figs 3*F*, 4*C* and 5*B*. For determining decays due to endocytosis, the average trace recorded in cells perfused with 200 μm l^{-1} cadmium was subtracted prior to fitting the poststimulus decay in capacitance with a non-linear least squares fitting algorithm as previously described (Engisch & Nowycky, 1998).

Amperometric traces were imported into Origin (OriginLab Corp., Northampton, MA, USA) for display. Subjective criteria were used for counting the number of events during a train, to include slow and/or small amplitude events typically missed with an automated peak detection algorithm. Two investigators judged each trace to minimize false positives. Events may have been undercounted when numbers reached > 20, since slower, smaller events are only easily detected on a flat baseline.

Data in all figures are presented as means ± S.E.M. Single point statistical comparisons were made using Student's *t* test; $P < 0.05$ was considered statistically significant.

Results

Rab3AQ81L strongly inhibits exocytosis evoked by repetitive stimulation

We used the capacitance detection method to follow increases in cell surface area due to exocytosis. Recordings were performed in perforated patch voltage clamp mode, to preserve the intracellular milieu and prevent secretory run down (Gillis *et al.* 1991; Engisch & Nowycky, 1996). Two days after infecting bovine chromaffin cells with a Rab3AQ81L–IRES–GFP adenovirus (see Methods), we observed variable amounts of green fluorescence in live cells. Coexpression of Rab3AQ81L and GFP was confirmed in fixed cells with an anti-HA antibody to recognize the HA-tagged Rab3A mutant (data not shown). Cells infected with a GFP–IRES–β-galactosidase adenovirus served as controls. Low levels of Rab3AQ81L expression, corresponding to dim GFP fluorescence,

did not affect depolarization-evoked exocytosis (data not shown). All the data are from cells with bright GFP fluorescence. Although fluorescence levels were not quantitatively determined, 'dim' refers to fluorescence that is just barely detectable above the background fluorescence/autofluorescence observed in uninfected cells; 'bright' refers to fluorescence that is still bright green when the visible light source is on. It is likely that dim and bright cells differ in amounts of Rab3AQ81L and GFP by 4- to 15-fold. The control virus also had effects when expressed at bright levels but not at dim levels; bright GFP-positive cells had smaller amplitude calcium currents and were more likely to show positive modulation during repetitive stimulation than untreated cells. These findings will appear elsewhere (R. Thiagarajan & K. L. Engisch, unpublished observations).

Chromaffin cells were stimulated with a series of 10 ms depolarizations at an interval of 200 ms, a protocol that

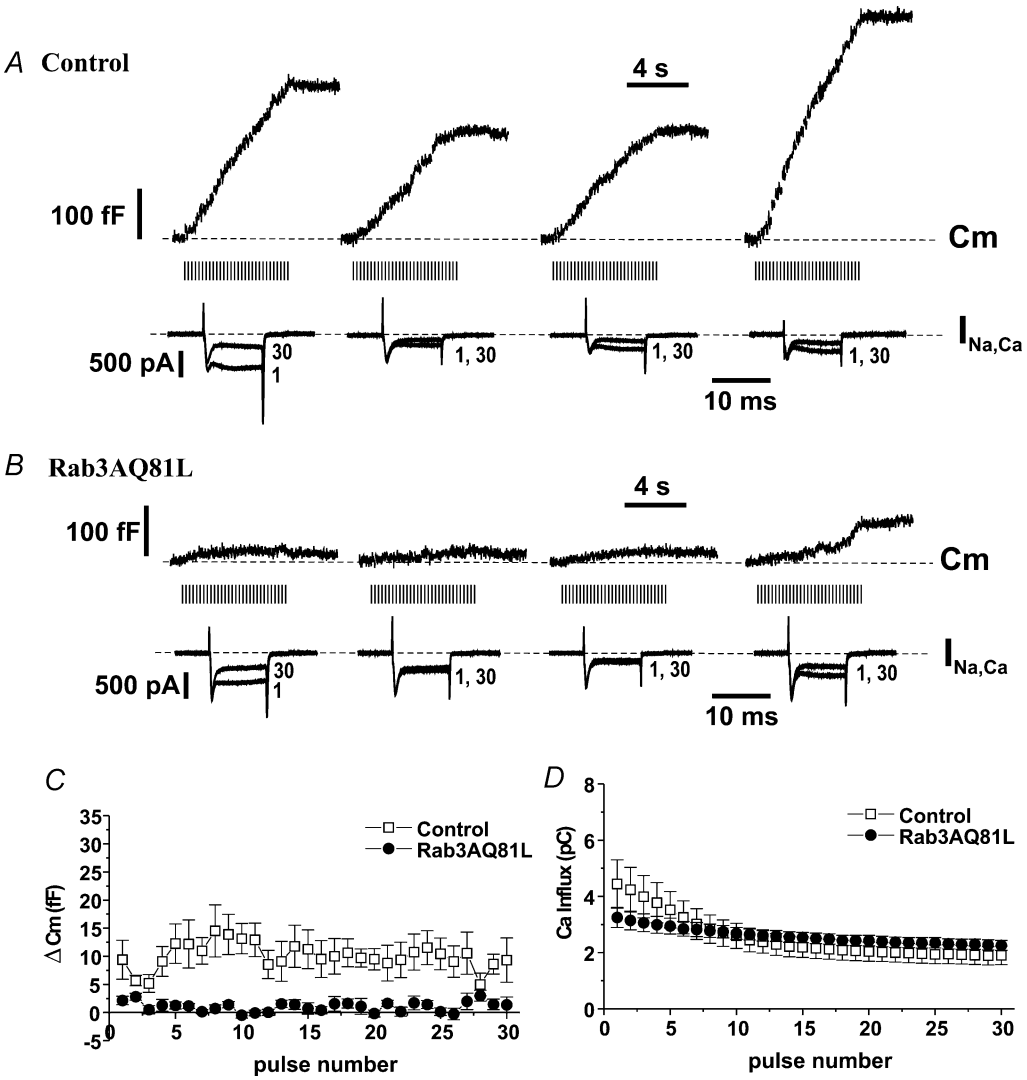

Figure 1. Exocytosis during repetitive stimulation is strongly inhibited in bovine adrenal chromaffin cells expressing Rab3AQ81L

A, capacitance (C_m) and first and last inward currents ($I_{Na,Ca}$) recorded during stimulation with a train of 10 ms depolarizations (30 pulses, −90 mV to +20 mV, 200 ms interval between pulses) in four different bovine chromaffin cells infected with control adenovirus (GFP–IRES–β-galactosidase). Bars under the C_m traces indicate timing of depolarizations. Dashed lines indicate initial C_m or holding current. *B*, C_m and $I_{Na,Ca}$ recorded during stimulation with a train of 10 ms depolarizations in four different bovine chromaffin cells infected with Rab3AQ81L adenovirus (Rab3AQ81L–IRES–GFP). *C*, average C_m response (ΔC_m) for each pulse of the train in control and Rab3AQ81L-expressing cells. *D*, average calcium influx (calculated from integral of calcium current) for each pulse of the train. $n = 9$ and 10 cells for control and Rab3AQ81L, respectively. $[Ca^{2+}]_o = 5$ mmol l^{-1}. Error bars are ± S.E.M.

Table 1. Comparison of capacitance responses (ΔC_m; fF) triggered by the first and tenth pulse of a train in control cells, Rab3AQ81L-expressing cells and Rab3AWT-expressing cells

	10 ms pulses		40 ms pulses	
Adenoviral construct	1st pulse	10th pulse	1st pulse	10th pulse
Control	9.4 ± 3.5	13.2 ± 2.7	22.8 ± 4.5	21.0 ± 5.7
Rab3AQ81L	2.1 ± 0.7*	−0.5 ± 0.5*†	10.4 ± 1.2*	0.1 ± 1.9*†
Control	6.1 ± 1.9	9.3 ± 2.4	16.6 ± 2.9	18.9 ± 3.6
Rab3AWT	2.5 ± 0.6	3.7 ± 1.0*	11.6 ± 1.9	2.2 ± 1.0*†

Controls are cells from the same cultures, infected with control adenovirus (GFP–IRES–β-galactosidase). *$P < 0.05$ *versus* control; †$P <$ 0.05 *versus* 1st pulse of the same train.

induces activity-dependent enhancement of exocytosis in ∼30% of untreated control cells (Engisch *et al.* 1997, 1999*a*,*b*). The repetitive stimulation protocol evoked large cumulative increases in capacitance (C_m) in control, virus-infected cells (Fig. 1*A*; each trace from a different cell), but much smaller capacitance increases in cells expressing Rab3AQ81L (Fig. 1*B*). This result is consistent with previous studies showing a dramatic reduction in hormone release in bovine chromaffin cells expressing Rab3AQ81L (Holz *et al.* 1994; Johannes *et al.* 1994; Chung *et al.* 1999).

Our goal was to determine if inhibition of exocytosis by Rab3AQ81L was activity-dependent. In Fig. 1*C* we plotted the average capacitance jump for each pulse in the train for control and Rab3AQ81L-expressing cells. Two phases of activity-dependent modulation were apparent in control cells. Over the first three depolarizations, the size of the capacitance jump declined, indicating activity-dependent depression. Response amplitude then returned gradually to initial levels between pulse 5 and 10, indicating activity-dependent facilitation. In contrast, Rab3AQ81L-expressing cells only responded to the first two depolarizations. Responses did not show the second phase of modulation, the facilitation phase, and were essentially zero for the rest of the train. We assessed the change in activity-dependent modulation caused by Rab3AQ81L expression by comparing the responses to the first and tenth pulse within a train (Table 1). In control cells, the first and tenth responses were not significantly different from each other. This is because facilitation causes response amplitude to recover to initial values. In Rab3AQ81L-expressing cells, the tenth response was significantly less than the first response, because response amplitude declined and never recovered.

Calcium current inactivation is not a factor in activity-dependent inhibition

Perforated patch recordings allow us to examine the contribution of calcium current modulation to effects of Rab3AQ81L on exocytosis. Chromaffin cells displayed variable amounts of calcium current inactivation during a train of 10 ms pulses (Fig. 1*A* and *B*), but on average Rab3AQ81L-expressing cells displayed less inactivation (Fig. 1*D*). Therefore the almost total inhibition of vesicle fusion during repetitive stimulation in Rab3AQ81L-expresssing cells cannot be explained by a greater inactivation of calcium currents. Less inactivation of calcium currents in Rab3AQ81L-expressing cells was not due to altered Na^+ current kinetics because only a fast inward current remained in the presence of 200 μmol l^{-1} cadmium (data not shown).

A decrease in Rab3A activity appears to lower the threshold calcium requirement for exocytosis (Johannes *et al.* 1996). Therefore, the calcium requirement for triggering exocytosis might be increased in cells expressing Rab3AQ81L, which is presumably in the active, GTP-bound conformation. If calcium influx falls below the higher threshold when calcium currents inactivate during repetitive stimulation, exocytosis would decrease and perhaps cease in what would appear to be an activity-dependent manner. To rule out this explanation for the decline in exocytosis in Rab3AQ81L-expressing cells during repetitive stimulation, we raised calcium influx by increasing the pulse duration to 40 ms. Calcium influx for every depolarization in a train of 40 ms pulses was higher than calcium influx for the first pulse of a train of 10 ms pulses (compare Fig. 1*D* with Fig. 2*D*). If the only reason responses declined to zero during a train of 10 ms pulses was that calcium influx fell below a threshold requirement, then during the train of 40 ms pulses, every response should be at least as large as the response to the first pulse of a train of 10 ms pulses.

In a Rab3AQ81L-expressing cell, a train of twenty 40 ms pulses evoked a cumulative increase in capacitance of less than 20 fF (Fig. 2*B*). In contrast, the cumulative increase in capacitance evoked in a control cell by the same stimulation was more than 300 fF (Fig. 2*A*). Figure 2*C* shows the average responses for each pulse of the train. We found that in Rab3AQ81L-expressing cells, response amplitude

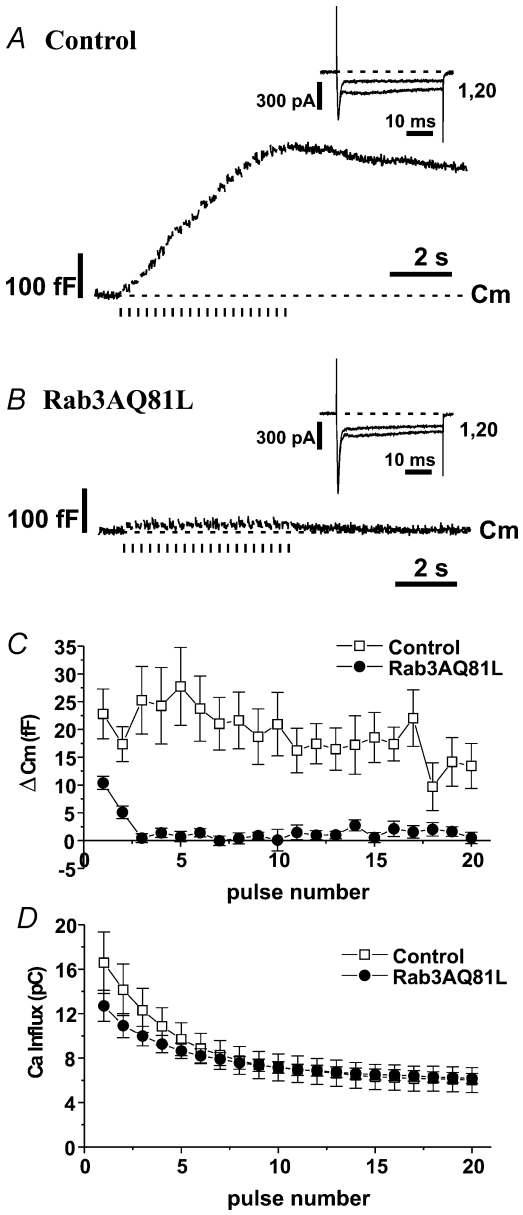

Figure 2. Increasing calcium influx by changing pulse duration from 10 to 40 ms did not prevent rapid cessation of exocytosis during a train in Rab3AQ81L-expressing cells

A, representative capacitance response (C_m) recorded in a bovine adrenal chromaffin cell infected with control adenovirus (GFP–IRES–β-galactosidase), during stimulation with a train of 40 ms depolarizations (20 pulses, −90 mV to +20 mV, 200 ms interval between pulses). *B,* representative C_m recorded in a cell infected with Rab3AQ81L adenovirus (Rab3AQ81L–IRES–GFP), during stimulation with a train of 40 ms depolarizations. Insets, first and last inward currents ($I_{Na,Ca}$). *C,* average C_m response (ΔC_m) for each pulse of the train in control and Rab3AQ81L-expressing cells. *D,* average calcium influx for each pulse of the train. $n = 10$ and 9 cells for control and Rab3AQ81L, respectively. $[Ca^{2+}]_o = 5$ mmol l^{-1}. Error bars are ± S.E.M.

remained close to zero after the second pulse. This lack of exocytosis appears to be due to something other than inadequate calcium influx, because 2–3 fF can be evoked by less calcium influx when that influx occurs on the first pulse of a (10 ms) train.

Rab3AQ81L modestly inhibits exocytosis evoked by single depolarizations

Depletion of fusion competent vesicles in Rab3AQ81L-expressing cells, but not in control cells, could explain a widening gap in exocytosis between the two groups as stimulation continued during a train. A limited pool of vesicles has been suggested when exocytosis evoked by a single depolarization reaches a plateau as pulse duration is increased (Horrigan & Bookman, 1994; Gillis *et al.* 1996; Sun & Wu, 2001). To determine whether the declining response in Rab3AQ81L-expressing cells during repetitive stimulation was due to reduction in the size of a releasable pool, we stimulated cells with depolarizations of duration 10, 40, 160 and 320 ms, in a 5 mmol l^{-1} $CaCl_2$ solution. Capacitance traces recorded in a control cell are shown in Fig. 3*A*, along with responses evoked by 320 ms depolarizations in 2.5 mmol l^{-1} $CaCl_2$ and 1 mmol l^{-1} $CaCl_2$ solutions. Figure 3*B* shows the responses evoked by the same stimuli in a cell expressing Rab3AQ81L. We have previously shown that capacitance responses are a function of calcium influx rather than duration (Engisch & Nowycky, 1996), and in Fig. 3*E* we have plotted capacitance responses *versus* calcium influx for 320 and 40 ms depolarizations applied in different concentrations of external calcium. For each value of calcium influx, the response of the Rab3AQ81L-expressing cell was smaller than that of the control cell, but a clear plateau was not observed in either relationship. The results from the two selected cells were representative of the population as a whole, as shown in Fig. 3*F*. The larger range of calcium influx in control cells can be attributed to a small number of cells with unusually large calcium currents ($N = 4$ for the last bin of control data).

We found that exocytosis increased linearly with calcium influx up to the highest values of calcium influx achieved. Figure 3*F* shows linear regression fits of the data (continuous line, control; dashed line, Rab3AQ81L), and both the slope and the *y*-intercept were reduced in cells expressing Rab3AQ81L (slope, 0.65 fF pC^{-1}, *y*-intercept, 0.5 fF; control, slope, 1.2 fF pC^{-1}, *y*-intercept, 6.0 fF). In addition to the relationships being well described by straight lines (*R*-value 0.99, where *R* is the correlation coefficient), the ratio of the Rab3AQ81L response to the control response did not decrease with increasing

calcium influx. The ratio was smallest for the least amount of calcium influx (bin 1, $\Delta C_{m,Rab3AQ81L}/\Delta C_{m,Control} = 0.4$), and ranged between 0.5 and 0.55 for the other bins. These data indicate that the deviation between control and Rab3AQ81L responses does not increase with stimulus strength, and therefore it does not appear that the Rab3AQ81L responses are prematurely approaching a plateau. However, we cannot rule out that the ~50% decrease in exocytosis is due to a smaller releasable pool in Rab3AQ81L-expressing cells that would be revealed if we could achieve higher amounts of calcium influx. It would be difficult to increase calcium influx further, as cells were bathed in a solution containing 5 mmol l^{-1} $CaCl_2$. Calcium current saturates between 5 and 10 mmol l^{-1} $[Ca^{2+}]_o$ (R. Thiagarajan & K. L. Engisch, unpublished observations; Xu & Adams, 1992). Alternatively, flash photolysis of a

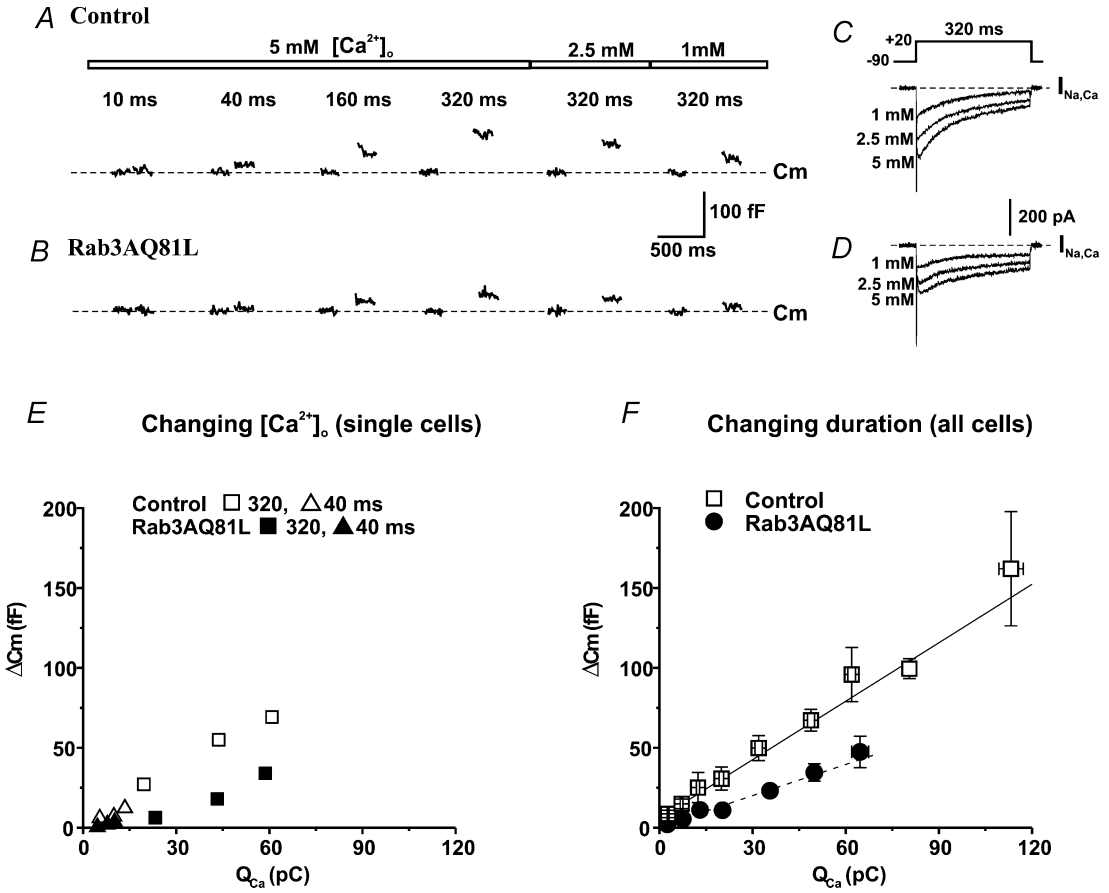

Figure 3. The slope of the calcium influx–exocytosis relationship is decreased in cells expressing Rab3AQ81L

A, capacitance responses (C_m) recorded in a cell infected with control virus (GFP–IRES–β-galactosidase). Shown are the 200 ms before and the 200 ms after a depolarization (−90 mV to +20 mV); gaps occur where phase tracking was suspended during the depolarization. Pulse duration is indicated above the traces; the numbers above the bars indicate the calcium concentrations in the extracellular solution. *B,* C_m responses to the same stimuli as in *A*, recorded in a cell infected with Rab3AQ81L adenovirus (Rab3AQ81L–IRES–GFP). *C* and *D,* inward current traces recorded during the 320 ms depolarizations in 5, 2.5 and 1 mmol l^{-1} $[Ca^{2+}]_o$ in the control cell and Rab3AQ81L-expressing cell from *A* and *B*, respectively. *E,* ΔC_m plotted as a function of calcium influx for 320 ms (squares) and 40 ms depolarizations (triangles) in 5, 2.5 and 1 mmol l^{-1} $[Ca^{2+}]_o$ for the control cell from *A* (open symbols) and the Rab3AQ81L-expressing cell from *B* (filled symbols). *F*, average ΔC_m *versus* calcium influx for 10, 40, 160 and 320 ms depolarizations in 5 mmol l^{-1} $[Ca^{2+}]_o$. $n = 24$ cells for control and 24 cells for Rab3AQ81L. Data were sorted by amount of calcium influx, divided into bins, and the mean C_m response of each bin plotted *versus* the mean calcium influx of each bin. No more than one value at a given duration is included per cell. Bin *N* ranges from 4 to 16 for control and 5–23 for Rab3AQ81L. Lines are linear regression fits to the data (control, continuous line; slope = 1.2 fF pC^{-1}, *y*-intercept = 6.0 fF, $R = 0.99$; Rab3AQ81L, dashed line; slope = 0.65 fF pC^{-1}, *y*-intercept = 0.5 fF, $r = 0.99$). Error bars are ± S.E.M.

photolabile calcium chelator could increase intracellular calcium to higher levels (Heinemann *et al.* 1994). It would be informative to use flash photolysis to determine if expression of Rab3AQ81L reduces the size of the first component of the exocytotic burst, which was recently demonstrated to correspond to the readily releasable pool (Voets *et al.* 1999).

More importantly, the maximal capacitance response evoked by a single depolarization in Rab3AQ81L-expressing cells, 47 fF, was many times greater than what could be elicited by the initial pulses of a train of depolarizations prior to depression, ∼5 fF for the first two 10 ms pulses of a train; ∼15 fF for the first two 40 ms pulses of a train (see Figs 1*C* and 2*C*). Therefore the lack of response after the first several pulses of a stimulus train in Rab3AQ81L-expressing cells cannot be explained by simple depletion of a smaller pool of releasable vesicles.

Wild-type Rab3A inhibits exocytosis during repetitive stimulation

The inhibitory effects of Rab3AQ81L on exocytosis during repetitive stimulation could be caused by an increase in Rab3A function, or by interference of Rab3A function in a dominant negative manner. In previous studies, expression of wild-type Rab3A (Rab3AWT) either inhibited hormone release (Holz *et al.* 1994; Weber *et al.* 1996; Smith *et al.* 1997; Chung *et al.* 1999; Schluter *et al.* 2002), or had no effect (Regazzi *et al.* 1996; Coppola *et al.* 1999; Iezzi *et al.* 1999). These data support the assumption that Rab3AQ81L is the activated form of Rab3A. We examined whether overexpression of wild-type Rab3A in bovine chromaffin cells caused a similar activity-dependent inhibition of exocytosis. We infected chromaffin cells with a Rab3AWT–IRES–GFP adenovirus, and 48 h after infection recorded capacitance increases evoked by repetitive stimulation. Controls were cells from the same culture, infected with the GFP–IRES–β-galactosidase virus.

Responses evoked in Rab3AWT-expressing cells by repetitive stimulation with 10 ms (Fig. 4*A*) or 40 ms depolarizations (Fig. 4*B*) followed the patterns we observed in Rab3AQ81L-expressing cells. During the facilitation phase, the increase in response amplitude was severely blunted for both protocols, with responses significantly smaller than those of control cells at the tenth pulse of each train (Table 1). These results show that impaired GTPase activity and a reduced ability to interact with a guanine nucleotide releasing factor (GRF; Brondyk *et al.* 1993) are not necessary for activity-dependent inhibition of exocytosis by Rab3A.

Although the effects of wild-type Rab3A were in the same direction as those of the GTPase-deficient mutant, there were important differences. Rab3AWT had a smaller inhibitory effect on the response to the first pulse of a

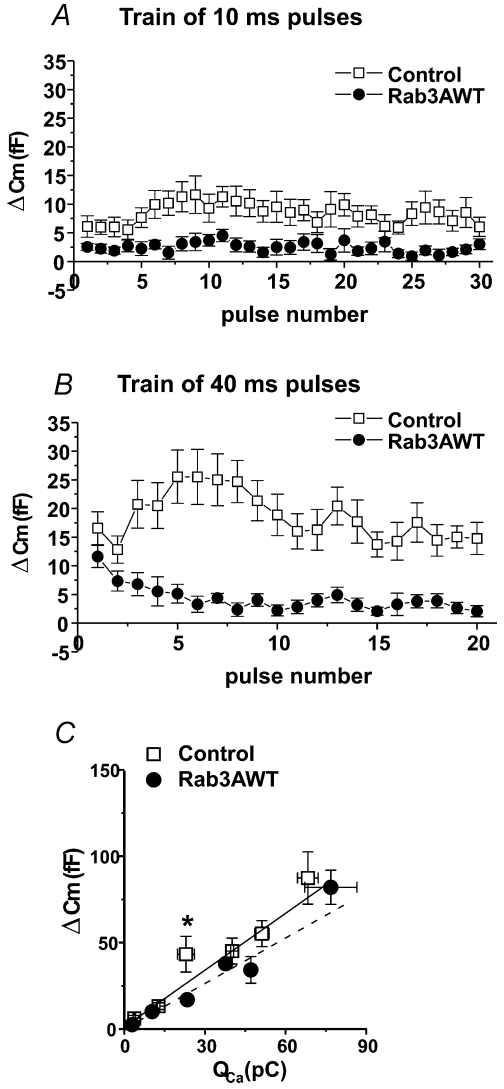

Figure 4. Adenoviral-induced expression of wild-type Rab3A (Rab3AWT) in bovine adrenal chromaffin cells inhibits exocytosis evoked by repetitive stimulation but has little effect on the calcium influx-exocytosis relationship

A, average C_m response (ΔC_m) for each pulse of a train of 10 ms depolarizations (−90 mV to +20 mV, 200 ms between pulses) in control (open symbols, $n = 10$) and Rab3AWT-expressing cells (filled symbols, $n = 12$). *B*, average ΔC_m for each pulse of a train of 40 ms depolarizations in control ($n = 11$) and Rab3AWT-expressing cells ($n = 12$). *C,* calcium influx–exocytosis relationships for control ($n = 11$) and Rab3AWT-expressing cells ($n = 14$), generated as described in Fig. 3 legend. (*N* for bins ranges between 5 and 12 for both control and Rab3AWT.) Lines are linear regression fits to the data. Control, continuous line; slope = 1.1 fF pC^{-1}, *y*-intercept = 1.2 fF, $R = 0.98$; Rab3AWT, dashed line; slope = 0.9 fF pC^{-1}, *y*-intercept = −0.04 fF, $R = 0.99$. $^*P < 0.05$ *versus* control bin. $[Ca^{2+}]_o = 5$ mmol l^{-1}. Error bars are ± S.E.M.

train, which did not reach statistical significance, due in part to smaller control responses in this group of cells (10 ms pulses, $P = 0.07$; 40 ms pulses, $P = 0.16$; Table 1). In Rab3AWT-expressing cells, response amplitude was significantly different from zero at the tenth pulse ($P < 0.05$ for 10 and 40 ms pulses); it was not in Rab3AQ81L-expressing cells ($P = 0.4$, 0.9 for 10 and 40 ms pulses, respectively). In Rab3AWT-expressing cells, the response to the tenth pulse was significantly different from the response to the first pulse within the same train for a train of 40 ms pulses, but not for a train of 10 ms pulses (Table 1). It is unlikely that the quantitative difference in the extent of inhibition can be explained by lower amounts of overexpressed protein in the cells infected with the wild-type Rab3A adenovirus, since GFP fluorescence was used to choose cells in both experiments, and there is no reason to suspect a systematically lower fluorescence in the Rab3AWT group. Another indication of similar virus levels in both groups is the comparable calcium influx, 2.9 pC for first 10 ms pulse in Rab3AWT-expressing cells and 3.3 pC in Rab3AQ81L-expressing cells ($P = 0.48$), indicating infection with a similar amount of virus, which causes calcium current inhibition. Finally, no difference in Rab3A-specific immunoreactivity was observed in confocal images of Rab3A immunofluorescence in Rab3AWT- and Rab3AQ81L-expressing cells (R. Thiagarajan & K. L. Engisch, unpublished observations). These results do not support the idea that the effects of Rab3AQ81L and Rab3AWT are due to bulk interference, since they were expressed at similar amounts and only differ by a single amino acid substitution.

Given the small effect of Rab3AWT on the first pulse of a stimulus train, we did not expect the calcium influx–exocytosis relationship to be altered in Rab3AWT-expressing cells. Responses to single depolarizations of 10–320 ms duration were sorted by amount of calcium influx and binned into groups as described for Fig. 3*F*. The average capacitance responses for each bin are plotted in Fig. 4*C*. The slope and *y*-intercept for Rab3AWT-expressing cells were slightly smaller than those of control cells (dashed line, Rab3AWT, slope 0.88 fF pC^{-1}, *y*-intercept −0.04 fF; continuous line, control, slope 1.1 fF pC^{-1}; *y*-intercept 1.2 fF). A comparison of response amplitudes found a significant difference only for the third bin (asterisk in Fig. 4*C*). These data show that expression of wild-type Rab3A causes strong activity-dependent inhibition and a much smaller effect on 'resting' exocytosis.

Rab5A has no effect on activity-dependent modulation or calcium sensitivity

Inhibition of hormone release has been observed in previous studies that used other methods of gene transduction, suggesting our results are not due to adenovirus *per se*. In addition, cells infected with the Rab3AQ81L adenovirus had levels of GFP fluorescence similar to cells infected with control virus, so it is unlikely our results are due to excessive amounts of GFP or viral proteins. However, we were concerned that in adenovirus-infected cells, levels of exogenous Rab3A or Rab3AQ81L might be high enough to cause secondary effects due to sequestration of Rab3A-interacting molecules.

In previous studies, some mutants of Rab3A did not inhibit release when expressed in chromaffin cells (Rab3AT36N and Rab3AV55E; Holz *et al.* 1994; Johannes *et al.* 1994). Furthermore, hormone release was not inhibited in PC12 cells expressing Rab3AQ81L with two additional mutations, R66L and R70T, that disrupt its interaction with calmodulin (Coppola *et al.* 1999; but see Schluter *et al.* 2002). These data suggest that inhibitory actions of Rab3A are specific because they only occur when Rab3A is in certain conformations that allow it to interact with downstream effectors. However, these mutants cannot be used to rule out sequestration of signalling molecules because they do not bind to downstream effectors and therefore would not be expected to sequester them.

To rule out that our effects were caused by sequestration of GTP/GDP regulators or cell signalling molecules, we expressed another active small GTPase, Rab5A, using adenovirus-mediated gene transfer. Rab5A regulates trafficking from the plasma membrane to early endosomes (see Zerial & McBride, 2001 for a recent review). Rab5 is localized to early endosomes in all cells, but a significant fraction of neuronal Rab5 is found on synaptic vesicles (de Hoop *et al.* 1994; Fischer von Mollard *et al.* 1994; Wucherpfennig *et al.* 2003). Rab5 interacts with the same GDP dissociation inhibitor (GDI) that regulates Rab3A (Ullrich *et al.* 1993), as well as being indirectly linked to calmodulin via early endosome antigen 1 (EEA1; (Mu *et al.* 1995; Mills *et al.* 2001). Rab5 also interacts with phosphatidylinositol-3-OH kinase (Christoforidis *et al.* 1999), a signalling molecule implicated in exocytosis (Chasserot-Golaz *et al.* 1998).

We infected chromaffin cells with an adenovirus that induced expression of Rab5A tagged with EGFP, and recorded capacitance increases evoked by repetitive

stimulation in fluorescent cells. Controls were cells infected with the GFP–IRES–β-galactosidase virus. During a train of 40 ms depolarizations, the responses in Rab5A-expressing cells overlapped exactly with responses in control cells from the same cultures: amplitudes initially declined, then increased (Fig. 5*A*). Untreated cells show a different pattern during repetitive stimulation: responses decline to a plateau value that is maintained for the duration of the train (R. Thiagarajan & K. L. Engisch, unpublished observations). A decline to a plateau is also observed for 'dim' cells from cultures infected with the GFP–IRES–β-galactosidase adenovirus (data not shown). The finding that cells infected with the Rab5–EGFP adenovirus show facilitation suggests they received virus levels comparable to 'bright' rather than 'dim' cells infected with GFP–IRES–β-galactosidase adenovirus. The calcium influx–exocytosis relationship was also unchanged in Rab5A-expressing cells (Fig. 5*B*). In sum, a small GTPase with a similar localization and repertoire of interacting proteins does not cause inhibition of exocytosis when

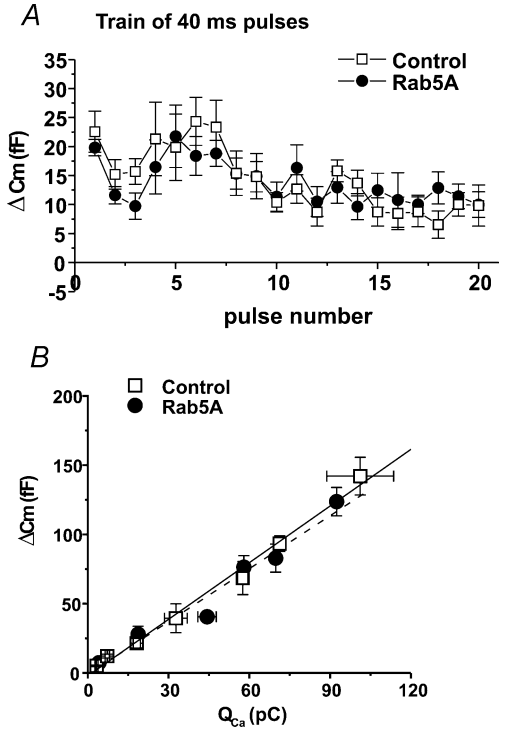

Figure 5. Adenoviral-induced expression of EGFP-tagged Rab5A in bovine adrenal chromaffin cells has no effect on exocytosis during a train of depolarizations, and no effect on the calcium influx–exocytosis relationship

A, average C_m response (ΔC_m) in control and Rab5A-expressing cells for each pulse of a train of 40 ms depolarizations (−90 mV to +20 mV, 200 ms between pulses). $n = 8$ and 9 cells for control and Rab5A, respectively. *B*, average ΔC_m *versus* calcium influx for 10, 40, 160 and 320 ms depolarizations ($n = 8$ cells for control and 10 cells for Rab5A). See Fig. 3 legend for details on generation of calcium influx-vesicle fusion relationship. (*N* for bins ranges between 3 and 5 for control and 4 and 10 for Rab5A.) Lines are linear regression fits to the data (control, continuous line; slope = 1.4 fF pC^{-1}, *y*-intercept = −2.1 fF, $R = 0.995$; Rab5A, slope = 1.3 fF pC^{-1}, *y*-intercept = −1.2 fF, $R = 0.98$). $[Ca^{2+}]_o = 5$ mmol l^{-1}. Error bars are ± S.E.M.

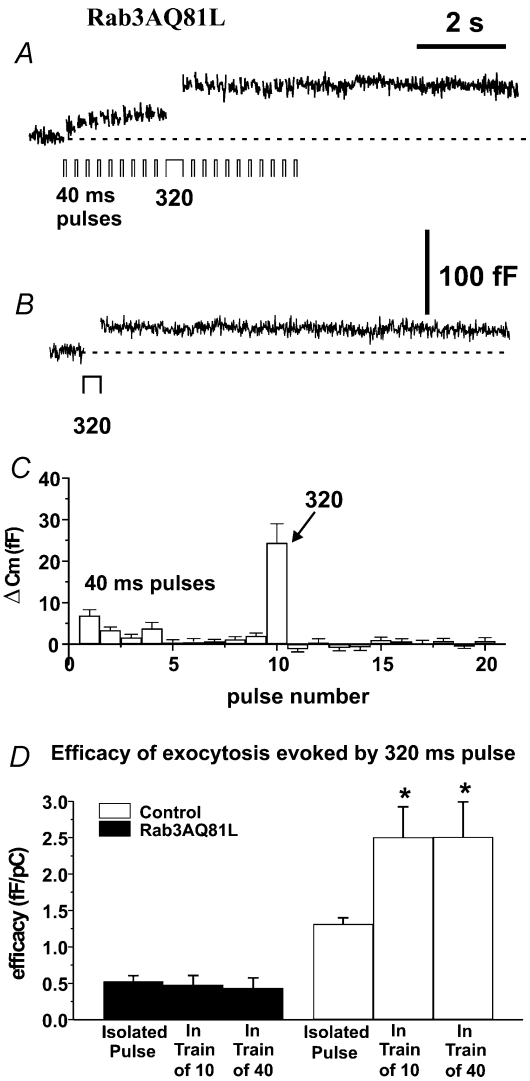

Figure 6. Rab3AQ81L-mediated inhibition does not increase during repetitive stimulation

A, representative capacitance (C_m) response recorded in a cell infected with Rab3AQ81L adenovirus (Rab3AQ81L–IRES–GFP) during stimulation with a train of 40 ms depolarizations, with duration increased to 320 ms on the tenth pulse. *B,* C_m recorded in the same cell during a single 320 ms pulse. *C,* average ΔC_m for each pulse of the modified train in Rab3AQ81L-expressing cells ($n = 15$ cells). *D*, the amount of exocytosis per calcium influx, or efficacy (fF pC^{-1}), was calculated for responses evoked by a single 320 ms pulse applied by itself ('isolated pulse'), during a train of 10 ms pulses ('in a train of 10'), and during a train of 40 ms pulses ('in a train of 40'), in control and Rab3AQ81L-expressing cells. $^*P < 0.05$ *versus* efficacy of isolated 320 ms pulse. $n = 18$ cells for control and 15 cells for Rab3AQ81L. Error bars are ± S.E.M.

expressed at high levels. These data suggest it is unlikely that excess amounts of any Rab GTPase would lead to activity-dependent inhibition, and support the hypothesis that the effects of Rab3A and Rab3AQ81L are specific.

Rab3AQ81L prevents positive modulation

There are two possible mechanisms that could lead to an increase in inhibition of exocytosis during repetitive stimulation in Rab3AQ81L- and Rab3AWT-expressing cells. Either repetitive stimulation boosts the inhibitory action of Rab3AQ81L/Rab3A, or Rab3AQ81L and Rab3A prevent positive modulation, i.e. facilitation. To distinguish between these possibilities, we inserted a large calcium influx pulse (320 ms) in the middle of a train of 10 or 40 ms pulses and stimulated Rab3AQ81L-expressing cells and control cells with the modified train. If Rab3AQ81L-mediated inhibition is increased by repetitive stimulation, the 320 ms depolarization within the train should trigger a smaller response than a 320 ms pulse applied without prior stimulation. Figure 6*A* shows a capacitance trace recorded in a Rab3AQ81L-expressing cell that was stimulated with a train of 40 ms depolarizations; the tenth pulse was a 320 ms depolarization. The brief depolarization evoked a capacitance increase only on the first pulse, but the 320 ms depolarization evoked a larger increase in capacitance than evoked by the initial 40 ms pulse. The response to a 320 ms depolarization during the train was similar to that evoked by an isolated 320 ms depolarization (Fig. 6*B*). The average capacitance jump for each pulse of the modified train is shown in Fig. 6*C*.

The data in Fig. 6*C* demonstrate that in a Rab3AQ81L-expressing cell, inhibition late in a train is incomplete, but does not rule out that Rab3AQ81L-mediated inhibition increases during the train. We compared 'efficacy', amount of exocytosis per amount of calcium influx in fF pC^{-1}, for 320 ms pulses inserted during trains, and isolated 320 ms pulses (Fig. 6*D*). We found that efficacy was the same whether the pulse was applied alone or during a train in Rab3AQ81L-expressing cells ($P = 0.7$, paired t test), indicating that inhibition did not increase during repetitive stimulation. In contrast, cells infected with control adenovirus showed a significant increase in efficacy for a 320 ms stimulus during a train of 10 or 40 ms pulses. This result indicates that repetitive stimulation induced facilitation in control cells, but not in Rab3AQ81L-expressing cells.

A possible explanation of our results is that Rab3AQ81L prevents $[Ca^{2+}]_i$ from rising to a level necessary to induce facilitation – perhaps by enhancing calcium extrusion, or by inhibiting calcium release from intracellular stores. To examine calcium concentration dynamics

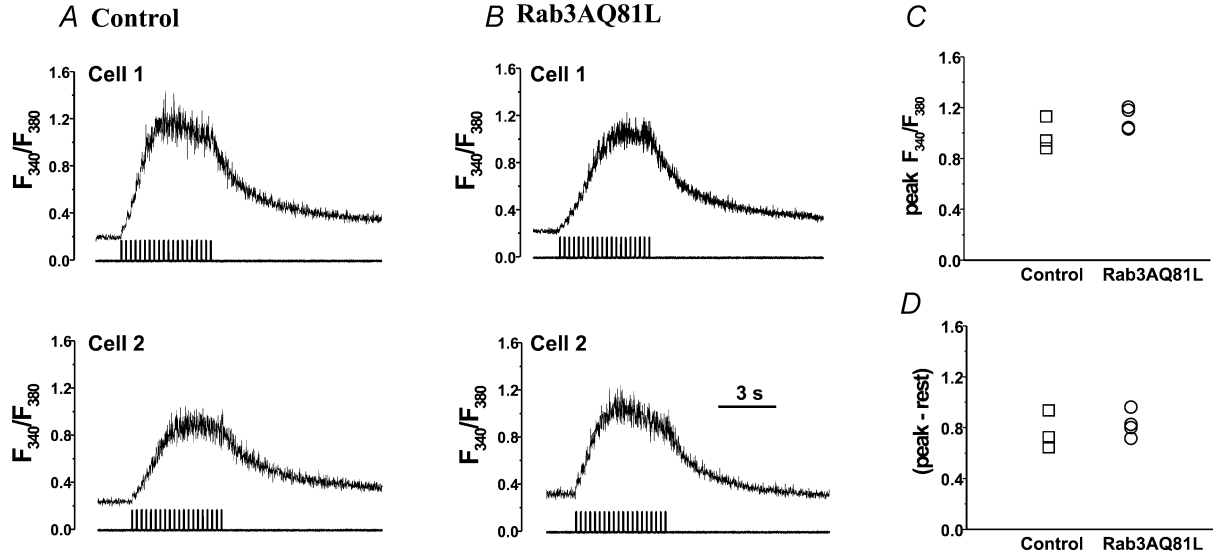

Figure 7. Expression of Rab3AQ81L does not alter global $[Ca^{2+}]_i$ dynamics during repetitive stimulation
A, perforated patch $[Ca^{2+}]_i$ recordings from two control cells infected with GFP–IRES–β-galactosidase adenovirus, stimulated with a train of 40 ms depolarizations (20 pulses, −90 to +20 mV, 200 ms interval between pulses). *B*, $[Ca^{2+}]_i$ recordings from two cells infected with Rab3AQ81L–IRES–GFP adenovirus. *C*, maximal background-corrected fluorescence ratio ('Peak') during the train for control ($n = 3$) and Rab3AQ81L-expressing cells ($n = 4$). *D*, maximal change in fluorescence ratio, determined from the difference between the peak fluorescence ratio and the ratio at rest, prior to stimulation. Cells were loaded by preincubation with 2 μm l^{-1} Fura-4F-AM.

during repetitive stimulation in control and Rab3AQ81L-expressing cells, we performed global intracellular calcium measurements using the ratiometric calcium indicator Fura-4F. We found that the global $[Ca^{2+}]_i$ dynamics during, and following, a train of 40 ms depolarizations were remarkably similar in a small sample of three control and four Rab3AQ81L-expressing cells. Fluorescence ratios from two control and two Rab3AQ81L-expressing cells are shown in Fig. 7*A* and *B*, respectively. The ratio accumulated with successive depolarizations, but reached a plateau between pulse 7 and 10. The plateau in $[Ca^{2+}]_i$ during repetitive stimulation is characteristic of chromaffin cells in the perforated patch configuration (Engisch *et al.* 1997). When stimulation ended, the ratio exponentially declined. The peak fluorescence ratios during the train were identical in the two groups (Fig. 7*C*, top), as was the maximum change in fluorescence ratio (peak minus the resting level; Fig. 7*D*). The rate that the fluorescence ratio increased, leading up to the plateau, was not lower in Rab3AQ81L-expressing cells (0.37 ± 0.03 ratio units s^{-1}, compared to 0.36 ± 0.09 ratio units s^{-1} in control cells), nor was the decay faster ($\tau = 2.09 \pm 0.24$ s, compared to 2.08 ± 0.15 s in control cells). These data suggest that expression of Rab3AQ81L did not cause changes in $[Ca^{2+}]_i$ handling that would lower global calcium concentration during repetitive stimulation, although we cannot rule out an alteration in calcium dynamics immediately beneath the membrane.

Rab3AQ81L and wild-type Rab3A inhibit asynchronous vesicle fusion

In cells infected with control adenovirus, capacitance often continued to increase for several seconds after a single 160 or 320 ms depolarization (Fig. 8*A*). Expression of Rab3AQ81L (Fig. 8*B*) or wild-type Rab3A virtually abolished poststimulus capacitance increases, but expression of Rab5A did not (Table 2). Post-stimulus capacitance increases are rare in untreated cells; usually the evoked capacitance increase is followed by a mono- or bi-exponential decrease corresponding to endocytosis (Fig. 8*C*; see also Artalejo *et al.* 1995; Smith & Neher, 1997; Engisch & Nowycky, 1998). It appears that increasing the amount of active Rab3A was able to reverse the change in calcium–secretion coupling that occurred after infection with adenovirus.

Does Rab3A inhibit endocytosis?

When rapid recycling of membrane is blocked in bovine adrenal chromaffin cells, exocytosis during subsequent periods of stimulation is progressively decreased (Elhamdani *et al.* 2001). If Rab3AQ81L inhibited rapid recycling, it might cause the type of decline in exocytosis we observed during repetitive stimulation. To examine endocytosis in cells expressing Rab3AQ81L we used a mono-exponential function to fit the decay of capacitance that occurs following single depolarizations, 320 ms in duration. In addition, we determined the amount of membrane recovered within 10 s of stimulation. We compared the results to those in untreated cells from the same cultures, because in adenovirus-infected cells, poststimulus exocytosis often obscured endocytosis. We did not determine endocytosis during repetitive stimulation as the interval between pulses, 200 ms, is too short for endocytosis to reach completion.

Table 2. Expression of Rab3AQ81L and Rab3AWT inhibits poststimulus vesicle fusion

Adenoviral construct	Cells with post-stimulus $\Delta C_m \geq 20$ fF	Post-stimulus ΔC_m (fF)*
Control	62% (13/21)	73 ± 12
Rab3AQ81L	0% (0/18)	—
Control	62% (5/8)	118 ± 42
Rab3AWT	15% (2/13)	22, 38
Control	50% (4/8)	49 ± 28
Rab5A-EGFP tag	67% (6/9)	59 ± 19

*Average post-stimulus ΔC_m when it occurs.

In Fig. 8*B*, the decay of capacitance following a 320 ms depolarization in a Rab3AQ81L-expressing cell has a time constant of 3.4 s (red curve). As mentioned in the beginning of Results, calcium currents were smaller in cells infected with adenovirus; similarly, calcium influx was significantly reduced in Rab3AQ81L-expressing cells compared to untreated cells for the responses used in analysis of endocytosis (51 ± 3 pC compared to 78 ± 5 pC in untreated cells, $P < 0.05$). For untreated cells, we also determined time constants of endocytosis for pulses of 160 ms duration, to compare responses with similar calcium influx (55 ± 4 pC). A capacitance response evoked in an untreated cell by a 160 ms depolarization is shown in Fig. 8*C*. The decay of capacitance following the depolarization is fitted with a time constant of 4.5 s (red curve). The average decay time constant in cells infected with the Rab3AQ81L adenovirus was 5.5 ± 0.9 s ($n = 15$), close to the median of the distribution of time constants in a previous group of untreated cells (Engisch & Nowycky, 1998), and not significantly different from the value for untreated cells from the same cultures (320 ms pulses, 4.5 ± 1 s, $n = 8$ cells; 160 ms pulses, 5.1 ± 0.5 s, $n = 7$ cells). In cells infected with the Rab3AQ81L adenovirus, almost 90% of the membrane added during exocytosis was retrieved within 10 s ($89 \pm 5.6\%$, $n = 18$), significantly

greater accuracy than exhibited by untreated cells (320 ms pulses, 63 ± 8%, $n = 12$; 160 ms pulses, 56 ± 7%, $n = 11$; $P < 0.05$). These results indicate that compensatory retrieval is not blocked in the presence of Rab3AQ81L, and it may be enhanced.

Since we found an apparent enhancement in the extent of endocytosis in Rab3AQ81L-expressing cells, it was possible that small or absent capacitance jumps during repetitive stimulation could be attributed to overlapping endocytosis, rather than a true decrease in exocytosis. Therefore we used the carbon fibre amperometric technique to directly measure catecholamine release. Figure 9*A* shows the capacitance trace (top) and amperometric trace (bottom) recorded from a representative control cell during stimulation with a train of 40 ms depolarizations. A cumulative capacitance increase of 518 fF was accompanied by 20 amperometric events. In a group of 14 control cells, the number of events during a train of 40 ms pulses ranged from 3 to 27 (mean = 9.7 ± 2.2). In contrast, repetitive stimulation of Rab3AQ81L-expressing cells failed to evoke amperometric events in 5/8 cells, and only 1 or 2 amperometric events in the other three cells (Fig. 9*B*). These data conclusively show that the lack of capacitance increase during repetitive stimulation in Rab3AQ81L-expressing cells is due to inhibition of exocytosis, rather than an increase in endocytosis.

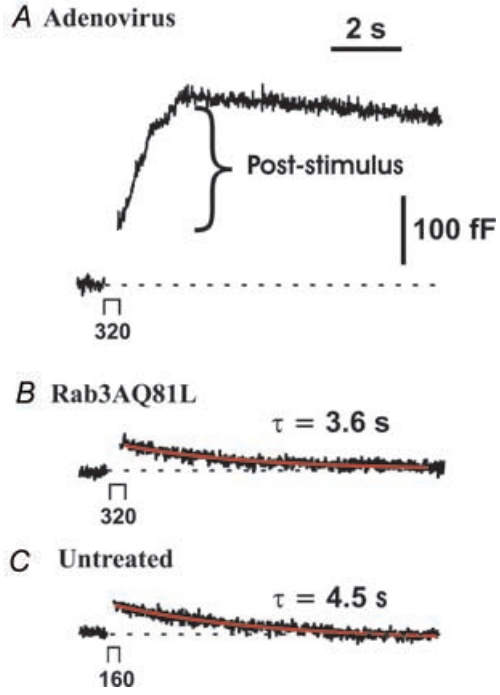

Figure 8. Expression of Rab3AQ81L inhibits poststimulus exocytosis, but endocytosis is similar to that of untreated cells
A, representative capacitance response (C_m) to a single 320 ms depolarization (−90 mV to +20 mV), recorded in a control cell infected with GFP–IRES–β-galactosidase adenovirus. In this response, the amount of poststimulus exocytosis (bracket) is greater than the C_m jump (capacitance increase immediately after gap in trace). *B*, representative C_m response evoked by a 320 ms depolarization in a cell infected with Rab3AQ81L–IRES–GFP adenovirus. *C*, C_m response evoked by a 160 ms depolarization in an untreated cell, chosen to match the amplitude of the response shown in *B*. The red traces represent non-linear least squares fit of the capacitance decay using a mono-exponential function (see Methods).

Discussion

We examined whether expression of a GTPase-deficient mutant of Rab3A, Rab3AQ81L, inhibits exocytosis in an activity-dependent manner. We found that exocytosis evoked by single depolarizations was modestly inhibited in bovine chromaffin cells expressing Rab3AQ81L. In the same cells, exocytosis evoked by pulses applied in rapid succession was completely blocked. Thus Rab3AQ81L-mediated inhibition appeared to increase during repetitive stimulation.

We performed a series of experiments to define the action of Rab3AQ81L. These took advantage of our ability to stimulate exocytosis repeatedly in a single cell during a perforated patch recording, while varying stimulation parameters such as pulse duration, calcium concentration, and number of stimuli. We could precisely measure the trigger for exocytosis, calcium influx, and detect both exocytosis and endocytosis by monitoring cell capacitance. We showed that the activity-dependent inhibition of exocytosis in Rab3AQ81L-expressing cells was not due to

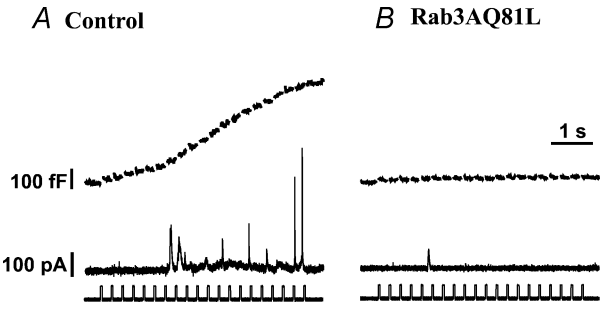

Figure 9. Catecholamine release detected with carbon fibre amperometry during a train of 40 ms depolarizations is strongly reduced by expression of Rab3AQ81L
A, capacitance trace (fF) and amperometric current (pA) simultaneously recorded in a control cell infected with the GFP–IRES–β-galactosidase adenovirus. The voltage protocol, 20 depolarizations, −90 mV to +20 mV, 200 ms intervals, is displayed below the amperometric trace. *B*, simultaneous capacitance and amperometric recordings in a cell infected with the Rab3AQ81L–IRES–GFP adenovirus.

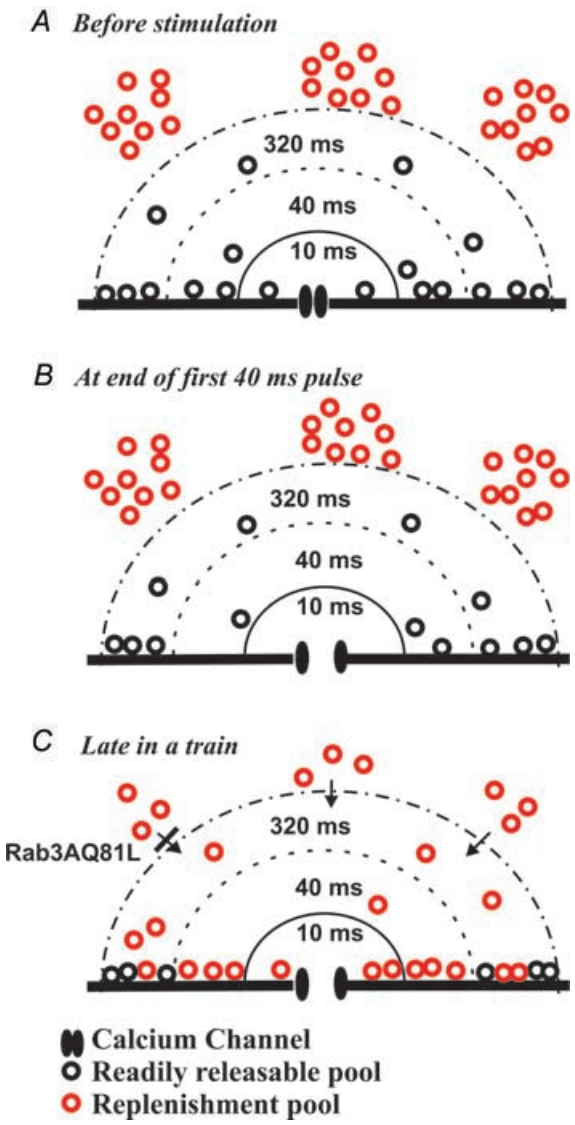

Figure 10. A model depicting how two vesicle pools may contribute to vesicle fusion during repetitive stimulation of bovine chromaffin cells

A, in the absence of stimulation, vesicles in the readily releasable pool (black) are distributed near the membrane, close to a calcium channel. Vesicles in the replenishment pool (red) are shown farther away, although their exact distribution has not been established. *B*, the first 40 ms pulse of a train depletes readily releasable vesicles from an area that experienced the increase in calcium concentration, which also includes the area that would be depleted by a 10 ms depolarization, rendered here as concentric half-circles around the calcium channel. Vesicles that are not touching the membrane are not released, but may approach the membrane, dock, and be released by subsequent stimuli. *C*, repetitive stimulation will cause build-up of calcium and diffusion toward the centre of the cell, where it can promote the mobilization of vesicles from the replenishment pool. After mobilization, the number of docked vesicles is larger than prior to stimulation, a possible explanation for increased efficacy (fF pC^{-1}). Inhibition of the recruitment or fusion of vesicles from the replenishment pool would explain the effects of Rab3AQ81L during repetitive stimulation.

greater calcium current inactivation, nor to calcium influx falling below a threshold calcium requirement. The rate of capacitance decay following single depolarizations was not decreased in Rab3AQ81L-expressing cells, indicating that endocytosis was functional and making it unlikely that activity-dependent depression was due to a failure to recycle vesicle membrane. We showed using carbon fibre amperometry that inhibition of capacitance jumps during repetitive stimulation was accompanied by inhibition of catecholamine release. The decline in exocytosis during repetitive stimulation was not due to simple depletion of release-ready vesicles, nor to an activity-dependent decrease in exocytotic efficacy for all fusion. Rather, an increase in exocytotic efficacy during repetitive stimulation that occurred in control cells was not observed in Rab3AQ81L-expressing cells. There was no alteration in intracellular calcium dynamics that could explain a lack of facilitation during repetitive stimulation. We conclude that Rab3AQ81L directly inhibits the mechanism(s) of activity-dependent facilitation.

Effects of Rab3AQ81L and Rab3A are the opposite of those caused by loss of Rab3A

We believe that the results observed in cells expressing Rab3AQ81L reveal the normal function of Rab3A, because expression of wild-type Rab3A similarly prevented facilitation of exocytosis during repetitive stimulation. This hypothesis would be strengthened if we could cause the opposite change by inhibiting Rab3A function. Although there are no dominant negative Rab3A mutants that stimulate transmitter release or promote activity-dependent facilitation, our hypothesis predicts that these effects should also occur when Rab3A is absent, as in a genetic deletion. Two findings in the Rab3A-knockout mouse agree with our prediction: there is facilitation rather than depression during a stimulus train at the diaphragm neuromuscular junction (Hirsh *et al.* 2002), and there is an increased amount of facilitation during a stimulus train at the Schaffer collateral–CA1 hippocampal synapse (Schoch *et al.* 2002). It has also been reported that the Schaffer collateral–CA1 synapse shows greater depression during repetitive stimulation in the Rab3A knockout (Geppert *et al.* 1994), a disparity in results that is difficult to explain since both studies examined the same synapse in slice recordings, although one looked at postsynaptic currents (Geppert *et al.* 1994) while the other recorded field potentials (Schoch *et al.* 2002). It is possible that multiple plasticity mechanisms overlap during a train. If the relative contribution of mechanisms involving Rab3A varies under different experimental

conditions, the effects due to loss of Rab3A may become obscured.

Our conclusion that Rab3A inhibits facilitation during a stimulus train is further supported by data from knockout mice lacking regulators of Rab3A GDP/GTP cycling and a putative downstream effector of Rab3A. Deletion in mice of a neuronal form of GDP dissociation inhibitor (GDI), guanine nucleotide exchange protein (GEP), or Rab3A-interacting molecule (RIM) in mice all lead to greater facilitation in CA1 hippocampal neurones during repetitive stimulation (Ishizaki *et al.* 2000; Schoch *et al.* 2002; Yamaguchi *et al.* 2002). The data from GDI-, GEP- and RIM-knockout mice must be interpreted with caution since these molecules are likely to regulate proteins other than Rab3A. However, the consistent increase in facilitation when Rab3A function is perturbed fits with our observation that augmenting Rab3A function decreases facilitation.

Darchen and coworkers previously examined the effects of Rab3A mutants on exocytosis in bovine chromaffin cells, using measurements of cell capacitance to follow exocytosis (Johannes *et al.* 1994). They found that the capacitance response was inhibited in cells injected with recombinant Rab3AQ81L protein. Because they used a 20 s depolarization as the stimulus for exocytosis they did not address whether Rab3AQ81L alters modulation during a stimulus train. In another experiment using the GTPase-deficient Rab3A mutant, it was found that transmitter release was reduced in cultured neurones from *Aplysia* injected with the *Aplysia* variant of Rab3AQ81L, Rab3AQ80L (Doussau *et al.* 1998). In contrast to our results, transmitter release showed facilitation, not depression, during repetitive stimulation. It is possible that the high rate of stimulation used in the *Aplysia* study (50 and 100 Hz) caused additional modulation processes involving Rab3A that are not present at the ∼5 Hz rate we used in chromaffin cells.

Rab3AQ81L-mediated inhibition of exocytosis during repetitive stimulation suggests the presence of two vesicle pools

In Rab3AQ81L-expressing cells that lack activity-dependent facilitation, the remaining activity-dependent depression is revealed. This depression had several surprising characteristics. First, exocytosis declined to zero in the same number of stimuli for both 10 and 40 ms depolarizations, despite a ∼3-fold greater amount of exocytosis evoked by the 40 ms depolarizations. Second, as stated in results, 3- to 10-fold greater exocytosis could be evoked by a single 320 ms depolarization. Thus the pool size, defined as the amount of exocytosis that can be achieved with strong stimulation in the absence of replenishment, appears to differ depending on the type of stimulus used. Figure 10 illustrates the model we propose to explain this behaviour. Prior to stimulation, vesicles are distributed throughout the cell, both near and far from a calcium channel (Fig. 10*A*). A 40 ms depolarization causes the calcium channel to open, resulting in an increase in calcium concentration in a region close to the channel; the vesicles in that region fuse (Fig. 10*B*). If another stimulus is applied, the area that experienced a rise in calcium is already depleted, and depression will be observed. If the first stimulus is a shorter depolarization, calcium increases over a smaller region and triggers fusion of fewer vesicles. But a second brief stimulus should cause depression with the same time course as the longer pulse, because repetitive stimulation either empties the small region or the large region.

Control cells show both depression and facilitation. To explain this result, we again use the model depicted in Fig. 10. In control cells, as in Rab3AQ81L-expressing cells, vesicles become depleted as the same stimulus is repetitively applied. But in control cells, something occurs to replenish the depleted region (Fig. 10*C*). We detect replenishment as facilitation when using a long pulse in the middle of a train, because the 320 ms pulse releases vesicles in a region not accessed by brief pulses, plus vesicles that have moved into the depleted region by a replenishment process. Replenishment probably depends on the build up of calcium and its spread away from the plasma membrane. Since Rab3AQ81L does not prevent a rise in global calcium, it must inhibit replenishment downstream from the calcium signal.

Because we measure fusion, the final step in a complex vesicle cycle, we cannot distinguish between the many possible means of replenishment, including recycling of previously exocytosed vesicles, priming of fusion-incompetent vesicles, or recruitment of vesicles from a storage depot. We favour the latter, and propose that replenishment is provided by vesicles in a slowly releasable pool, a pool first proposed to explain a slower rate of capacitance increase following a uniform rise in intracellular calcium (Heinemann *et al.* 1994; Voets *et al.* 1999). Slowly releasable vesicles do not fuse in response to single depolarizations up to 100 ms in duration (Voets *et al.* 1999; Voets, 2000), but fuse during repetitive stimulation with brief pulses applied at a rapid pace (2.5 Hz, Voets *et al.* 2001). It is likely that during the trains of 10 and 40 ms pulses used here, the vesicles fusing in response to the first pulses of the train are in the readily releasable pool, whereas those fusing late in a train are in the

slowly releasable pool. Rab3AQ81L and Rab3A inhibited exocytosis late in a train, and also the asynchronous release occurring after a long depolarization, which by definition had a slower time course than events occurring during the depolarization. In contrast, loss of synaptotagmin causes a selective inhibition of the readily releasable pool while the slowly releasable pool is preserved (Voets *et al.* 2001). Since the slowly releasable pool has primarily been defined using flash photolysis of caged calcium, it will be important to perform experiments using flash photolysis in Rab3AQ81L-expressing cells to support our hypothesis. Finally, it is unlikely that Rab3AQ81L acts at the final fusion step (Geppert *et al.* 1997), unless slowly releasable vesicles employ a fusion mechanism different from that of readily releasable vesicles.

We have demonstrated that inhibition of exocytosis by increased expression of Rab3AQ81L or Rab3AWT is activity-dependent. Our results, the opposite of those observed at synapses of the Rab3A-, GDI-, GEP- and RIM-knockout mice, bring together the seemingly divergent findings that the GTPase-deficient mutant blocks fusion while loss of Rab3A affects only activity-dependent modulation. We propose that Rab3A inhibits the recruitment of vesicles from a slowly releasable pool. This hypothesis has several implications for the interpretation of data in studies of Rab3A function. Forms of modulation involving the slowly releasable pool should be particularly sensitive to changes in Rab3A activity. Correspondingly, loss of Rab3A would not be expected to have any effect if the slowly releasable pool is not involved. Thus the wide variation in results across different neuronal populations in the Rab3A knockout (Castillo *et al.* 1997; Schoch *et al.* 2002) might be explained by the extent to which the slowly releasable pool participates during a particular pattern of activity in a given cell type. In addition, differences in Rab3A activity may contribute to variability in activity-dependent modulation between cells of the same population. Finally, Rab3A at endogenous levels may be an important brake on the slowly releasable pool, preventing its depletion in the face of prolonged repetitive stimulation, and cutting off asynchronous release after an impulse, to preserve the phase-locked kinetics that are the hallmark of fast transmitter release.

References

Artalejo CR, Henley JR, McNiven MA & Palfrey HC (1995). Rapid endocytosis coupled to exocytosis in adrenal chromaffin cells involves Ca^{2+}, GTP, and dynamin but not clathrin. *Proc Natl Acad Sci U S A* **92**, 8328–8332.

Brandt BL, Hagiwara S, Kidokoro Y & Miyazaki S (1976). Action potentials in the rat chromaffin cell and effects of acetylcholine. *J Physiol* **263**, 417–439.

Brondyk WH, McKiernan CJ, Burstein ES & Macara IG (1993). Mutants of Rab3A analogous to oncogenic Ras mutants. Sensitivity to Rab3A-GTPase activating protein and Rab3A-guanine nucleotide releasing factor. *J Biol Chem* **268**, 9410–9415.

Castillo PE, Janz R, Sudhof TC, Tzounopoulos T, Malenka RC & Nicoll RA (1997). Rab3A is essential for mossy fibre long-term potentiation in the hippocampus. *Nature* **388**, 590–593.

Castillo PE, Schoch S, Schmitz F, Sudhof TC & Malenka RC (2002). RIM1alpha is required for presynaptic long-term potentiation. *Nature* **415**, 327–330.

Chan SA & Smith C (2003). Low frequency stimulation of mouse adrenal slices reveals a clathrin-independent, protein kinase C-mediated endocytic mechanism. *J Physiol.* **553**, 707–717.

Chasserot-Golaz S, Hubert P, Thierse D, Dirrig S, Vlahos CJ, Aunis D & Bader MF (1998). Possible involvement of phosphatidylinositol 3-kinase in regulated exocytosis: studies in chromaffin cells with inhibitor LY294002. *J Neurochem* **70**, 2347–2356.

Chow RH, Klingauf J, Heinemann C, Zucker RS & Neher E (1996). Mechanisms determining the time course of secretion in neuroendocrine cells. *Neuron* **16**, 369–376.

Christoforidis S, Miaczynska M, Ashman K, Wilm M, Zhao L, Yip SC, Waterfield MD, Backer JM & Zerial M (1999). Phosphatidylinositol-3-OH kinases are Rab5 effectors. *Nat Cell Biol* **1**, 249–252.

Chung SH, Joberty G, Gelino EA, Macara IG & Holz RW (1999). Comparison of the effects on secretion in chromaffin and PC12 cells of Rab3 family members and mutants. Evidence that inhibitory effects are independent of direct interaction with Rabphilin3. *J Biol Chem* **274**, 18113–18120.

Clabecq A, Henry JP & Darchen F (2000). Biochemical characterization of Rab3-GTPase-activating protein reveals a mechanism similar to that of Ras-GAP. *J Biol Chem* **275**, 31786–31791.

Coppola T, Perret-Menoud V, Luthi S, Farnsworth CC, Glomset JA & Regazzi R (1999). Disruption of Rab3–calmodulin interaction, but not other effector interactions, prevents Rab3 inhibition of exocytosis. *EMBO J* **18**, 5885–5891.

Darchen F, Senyshyn J, Brondyk WH, Taatjes DJ, Holz RW, Henry JP, Denizot JP & Macara IG (1995). The GTPase Rab3a is associated with large dense core vesicles in bovine chromaffin cells and rat PC12 cells. *J Cell Sci* **108**, 1639–1649.

de Hoop MJ, Huber LA, Stenmark H, Williamson E, Zerial M, Parton RG & Dotti CG (1994). The involvement of the small GTP-binding protein Rab5a in neuronal endocytosis. *Neuron* **13**, 11–22.

Doussau F, Clabecq A, Henry JP, Darchen F & Poulain B (1998). Calcium-dependent regulation of rab3 in short-term plasticity. *J Neurosci* **18**, 3147–3157.

Elhamdani A, Palfrey HC & Artalejo CR (2001). Quantal size is dependent on stimulation frequency and calcium entry in calf chromaffin cells. *Neuron* **31**, 819–830.

Engisch KL, Chernevskaya NI & Nowycky MC (1997). Short-term changes in the Ca^{2+}-exocytosis relationship during repetitive pulse protocols in bovine adrenal chromaffin cells. *J Neurosci* **17**, 9010–9025.

Engisch KL & Nowycky MC (1996). Calcium dependence of large dense-cored vesicle exocytosis evoked by calcium influx in bovine adrenal chromaffin cells. *J Neurosci* **16**, 1359–1369.

Engisch KL & Nowycky MC (1998). Compensatory and excess retrieval: two types of endocytosis following single step depolarizations in bovine adrenal chromaffin cells. *J Physiol* **506**, 591–608.

Engisch KL, Rich MM, Cook N & Nowycky MC (1999*a*). Lambert-Eaton antibodies inhibit Ca^{2+} currents but paradoxically increase exocytosis during stimulus trains in bovine adrenal chromaffin cells. *J Neurosci* **19**, 3384–3395.

Engisch KL, Rich MM, Cook N & Nowycky MC (1999*b*). Lambert-Eaton antibodies promote activity-dependent enhancement of exocytosis in bovine adrenal chromaffin cells. *Ann N Y Acad Sci* **868**, 213–216.

Fidler N & Fernandez JM (1989). Phase tracking: an improved phase detection technique for cell membrane capacitance measurements. *Biophys J* **56**, 1153–1162.

Fischer von Mollard G, Mignery GA, Baumert M, Perin MS, Hanson TJ, Burger PM, Jahn R & Sudhof TC (1990). rab3 is a small GTP-binding protein exclusively localized to synaptic vesicles. *Proc Natl Acad Sci U S A* **87**, 1988–1992.

Fischer von Mollard G, Stahl B, Walch-Solimena C, Takei K, Daniels L, Khoklatchev A, De Camilli P, Sudhof TC & Jahn R (1994). Localization of Rab5 to synaptic vesicles identifies endosomal intermediate in synaptic vesicle recycling pathway. *Eur J Cell Biol* **65**, 319–326.

Geppert M, Bolshakov VY, Siegelbaum SA, Takei K, De Camilli P, Hammer RE & Sudhof TC (1994). The role of Rab3A in neurotransmitter release. *Nature* **369**, 493–497.

Geppert M, Goda Y, Stevens CF & Sudhof TC (1997). The small GTP-binding protein Rab3A regulates a late step in synaptic vesicle fusion. *Nature* **387**, 810–814.

Gillis KD, Mossner R & Neher E (1996). Protein kinase C enhances exocytosis from chromaffin cells by increasing the size of the readily releasable pool of secretory granules. *Neuron* **16**, 1209–1220.

Gillis KD, Pun RY & Misler S (1991). Long-term monitoring of depolarization-induced exocytosis from adrenal medullary chromaffin cells and pancreatic islet B cells using 'perforated patch recording'. *Ann N Y Acad Sci* **635**, 464–467.

Gonzalez M, Ruggiero FP, Chang Q, Shi YJ, Rich MM, Kraner S & Balice-Gordon RJ (1999). Disruption of Trkb-mediated signaling induces disassembly of postsynaptic receptor clusters at neuromuscular junctions. *Neuron* **24**, 567–583.

Heinemann C, Chow RH, Neher E & Zucker RS (1994). Kinetics of the secretory response in bovine chromaffin cells following flash photolysis of caged Ca^{2+}. *Biophys J* **67**, 2546–2557.

Hirsh JK, Searl TJ & Silinsky EM (2002). Regulation by Rab3A of an endogenous modulator of neurotransmitter release at mouse motor nerve endings. *J Physiol* **545**, 337–343.

Holz RW, Brondyk WH, Senter RA, Kuizon L & Macara IG (1994). Evidence for the involvement of Rab3A in Ca^{2+}-dependent exocytosis from adrenal chromaffin cells. *J Biol Chem* **269**, 10229–10234.

Horrigan FT & Bookman RJ (1994). Releasable pools and the kinetics of exocytosis in adrenal chromaffin cells. *Neuron* **13**, 1119–1129.

Iezzi M, Escher G, Meda P, Charollais A, Baldini G, Darchen F, Wollheim CB & Regazzi R (1999). Subcellular distribution and function of Rab3A, B, C, and D isoforms in insulin-secreting cells. *Mol Endocrinol* **13**, 202–212.

Ishizaki H, Miyoshi J, Kamiya H, Togawa A, Tanaka M, Sasaki T, Endo K, Mizoguchi A, Ozawa S & Takai Y (2000). Role of rab GDP dissociation inhibitor alpha in regulating plasticity of hippocampal neurotransmission. *Proc Natl Acad Sci U S A* **97**, 11587–11592.

Johannes L, Doussau F, Clabecq A, Henry JP, Darchen F & Poulain B (1996). Evidence for a functional link between Rab3 and the SNARE complex. *J Cell Sci* **109**, 2875–2884.

Johannes L, Lledo PM, Roa M, Vincent JD, Henry JP & Darchen F (1994). The GTPase Rab3a negatively controls calcium-dependent exocytosis in neuroendocrine cells. *EMBO J* **13**, 2029–2037.

Kawagoe KT, Zimmerman JB & Wightman RM (1993). Principles of voltammetry and microelectrode surface states. *J Neurosci Meth* **48**, 225–240.

Kraner SD, Rich MM, Sholl MA, Zhou H, Zorc CS, Kallen RG & Barchi RL (1999). Interaction between the skeletal muscle type 1 Na^+ channel promoter E-box and an upstream repressor element. Release of repression by myogenin. *J Biol Chem* **274**, 8129–8136.

Laflamme MA & Becker PL (1996). Ca^{2+}-induced current oscillations in rabbit ventricular myocytes. *Circ Res* **78**, 707–716.

Mills IG, Urbe S & Clague MJ (2001). Relationships between EEA1 binding partners and their role in endosome fusion. *J Cell Sci* **114**, 1959–1965.

Mu FT, Callaghan JM, Steele-Mortimer O, Stenmark H, Parton RG, Campbell PL, McCluskey J, Yeo JP, Tock EP & Toh BH (1995). EEA1, an early endosome-associated protein. EEA1 is a conserved alpha-helical peripheral membrane protein flanked by cysteine 'fingers' and contains a calmodulin-binding IQ motif. *J Biol Chem* **270**, 13503–13511.

Nassar-Gentina V, Pollard HB & Rojas E (1988). Electrical activity in chromaffin cells of intact mouse adrenal gland. *Am J Physiol* **254**, C675–C683.

Nonet ML, Staunton JE, Kilgard MP, Fergestad T, Hartwieg E, Horvitz HR, Jorgensen EM & Meyer BJ (1997). *Caenorhabditis elegans* rab-3 mutant synapses exhibit impaired function and are partially depleted of vesicles. *J Neurosci* **17**, 8061–8073.

Regazzi R, Ravazzola M, Iezzi M, Lang J, Zahraoui A, Andereggen E, Morel P, Takai Y & Wollheim CB (1996). Expression, localization and functional role of small GTPases of the Rab3 family in insulin-secreting cells. *J Cell Sci* **109**, 2265–2273.

Schluter OM, Khvotchev M, Jahn R & Sudhof TC (2002). Localization versus function of Rab3 proteins. Evidence for a common regulatory role in controlling fusion. *J Biol Chem* **277**, 40919–40929.

Schoch S, Castillo PE, Jo T, Mukherjee K, Geppert M, Wang Y, Schmitz F, Malenka RC & Sudhof TC (2002). RIM1alpha forms a protein scaffold for regulating neurotransmitter release at the active zone. *Nature* **415**, 321–326.

Seward EP & Nowycky MC (1996). Kinetics of stimulus-coupled secretion in dialyzed bovine chromaffin cells in response to trains of depolarizing pulses. *J Neurosci* **16**, 553–562.

Smith C (1999). A persistent activity-dependent facilitation in chromaffin cells is caused by Ca^{2+} activation of protein kinase C. *J Neurosci* **19**, 589–598.

Smith C & Neher E (1997). Multiple forms of endocytosis in bovine adrenal chromaffin cells. *J Cell Biol* **139**, 885–894.

Smith J, Thompson N, Thompson J, Armstrong J, Hayes B, Crofts A, Squire J, Teahan C, Upton L & Solari R (1997). Rat basophilic leukaemia (RBL) cells overexpressing Rab3a have a reversible block in antigen-stimulated exocytosis. *Biochem J* **323**, 321–328.

Sun J & Wu L (2001). Fast kinetics of exocytosis revealed by simultaneous measurements of presynaptic capacitance and postsynaptic currents at a central synapse. *Neuron* **30**, 171–182.

Ullrich O, Stenmark H, Alexandrov K, Huber LA, Kaibuchi K, Sasaki T, Takai Y & Zerial M (1993). Rab GDP dissociation inhibitor as a general regulator for the membrane association of rab proteins. *J Biol Chem* **268**, 18143–18150.

Vitale ML, Rodriguez Del Castillo A, Tchakarov L & Trifaro JM (1991). Cortical filamentous actin disassembly and scinderin redistribution during chromaffin cell stimulation precede exocytosis, a phenomenon not exhibited by gelsolin. *J Cell Biol* **113**, 1057–1067.

Voets T (2000). Dissection of three Ca^{2+}-dependent steps leading to secretion in chromaffin cells from mouse adrenal slices. *Neuron* **28**, 537–545.

Voets T, Moser T, Lund PE, Chow RH, Geppert M, Sudhof TC & Neher E (2001). Intracellular calcium dependence of large dense-core vesicle exocytosis in the absence of synaptotagmin I. *Proc Natl Acad Sci U S A* **98**, 11680–11685.

Voets T, Neher E & Moser T (1999). Mechanisms underlying phasic and sustained secretion in chromaffin cells from mouse adrenal slices. *Neuron* **23**, 607–615.

Weber E, Jilling T & Kirk KL (1996). Distinct functional properties of Rab3A and Rab3B in PC12 neuroendocrine cells. *J Biol Chem* **271**, 6963–6971.

Wucherpfennig T, Wilsch-Brauninger M & Gonzalez-Gaitan M (2003). Role of *Drosophila* Rab5 during endosomal trafficking at the synapse and evoked neurotransmitter release. *J Cell Biol* **161**, 609–624.

Xu ZJ & Adams DJ (1992). Voltage-dependent sodium and calcium currents in cultured parasympathetic neurones from rat intracardiac ganglia. *J Physiol* **456**, 425–441.

Yamaguchi K, Tanaka M, Mizoguchi A, Hirata Y, Ishizaki H, Kaneko K, Miyoshi J & Takai Y (2002). A GDP/GTP exchange protein for the Rab3 small G protein family up-regulates a postdocking step of synaptic exocytosis in central synapses. *Proc Natl Acad Sci U S A* **99**, 14536–14541.

Zerial M & McBride H (2001). Rab proteins as membrane organizers. *Nat Rev Mol Cell Biol* **2**, 107–117.

Zhou Z & Misler S (1995). Action potential-induced quantal secretion of catecholamines from rat adrenal chromaffin cells. *J Biol Chem* **270**, 3498–3505.

Acknowledgements

This work was supported by National Institutes of Health Grant MH64744. We thank Ian Macara for Rab3A cDNAs, Marino Zerial for Rab5A cDNA, and Allan Levey and Laura Volpicelli for EGFP-tagged Rab5A cDNA. We are grateful to Criss Hartzell and Lian Li for helpful comments on the manuscript.